

1 Learning and recognition of tactile temporal sequences by 2 mice and humans

3 Michael Bale^{1,2†}, Malamati Bitzidou^{2*}, Anna Pitas^{1,2*}, Leonie Brebner², Lina
4 Khazim², Stavros Anagnou², Caitlin Stevenson² and Miguel Maravall^{1,2†}

5 1 Instituto de Neurociencias UMH-CSIC, 03550 Sant Joan d'Alacant, Spain

6 2 Sussex Neuroscience, School of Life Sciences, University of Sussex, Brighton,
7 BN1 9QG, United Kingdom

8 * These authors contributed equally

9 † Corresponding authors

10 Abstract

11 The world around us is replete with stimuli that unfold over time. When we hear an auditory stream
12 like music or speech or scan a texture with our fingertip, physical features in the stimulus are
13 concatenated in a particular order, and this temporal patterning is critical to interpreting the stimulus.
14 To explore the capacity of mice and humans to learn tactile sequences, we developed a task in which
15 subjects had to recognise a continuous modulated noise sequence delivered to whiskers or fingertips,
16 defined by its temporal patterning over hundreds of milliseconds. GO and NO-GO sequences differed
17 only in that the order of their constituent noise modulation segments was temporally scrambled. Both
18 mice and humans efficiently performed tactile sequence learning. Mouse performance relied mainly
19 on detecting relative changes in noise amplitude over time, whereas humans appeared to have access
20 to more cues, including the duration of noise modulation segments.

21

22 Introduction

23 To make sense of the world around us, the brain must integrate sensory patterns and sequences over
24 time and assign them meaning. Signals in our environment unfold over time and can only be
25 interpreted by decoding their temporal patterning. The ability to do so underpins much of our sensory
26 experience – for example, it is central to recognising a favourite melody or a passage of speech [1]. As
27 first proposed over 60 years ago [2], sequence processing provides a model for investigating how
28 neuronal circuits give rise to object perception and recognition, a central goal of neuroscience [3, 4].

29 In tactile sensation, fast sensory events, such as fluctuations in the forces acting on a whisker follicle,
30 are encoded faithfully and with high temporal precision [5-11]. Exploring an object by scanning with
31 fingertips or whiskers generates a series of tactile events concatenated over time [12-17]. Recognising
32 the object as a whole – its texture, shape or size – requires integrating over these events, with the
33 relevant timescales varying from tens of milliseconds (ms) to seconds.

34 Introspection suggests that meaningful auditory sequences, such as those in speech or music, can be
35 learned quickly and robustly. We wondered whether similarly effective sequence learning and
36 recognition occurs in tactile sensory systems. We further wished to explore the cues that could
37 underlie capacities for tactile sequence recognition.

38 To address these issues, we developed a new experimental design for testing sequence discrimination
39 in mice and humans. Participants learn to distinguish a target stimulus sequence, constructed from an
40 underlying noise waveform, from other stimuli that differ only in their temporal patterning over
41 hundreds of milliseconds. Our results demonstrate efficient learning of tactile sequences both in mice
42 and in humans. This behaviour provides an assay for exploring the neuronal circuit mechanisms that
43 underpin recognition of temporally patterned stimuli.

44

45 Materials and Methods

46 Surgical procedures

47 All procedures were carried out in accordance with institutional, national (Spain and United Kingdom)
48 and international (European Union directive 2010/63/EU) regulations for the care and use of animals
49 in research. Details of head bar implantation surgery have been described elsewhere [7, 18]. Briefly,
50 under aseptic conditions, mice (male, total n = 32, 6-9 week old) were anaesthetised using 1.5-2.5%
51 isoflurane in O₂ and placed into a stereotaxic apparatus (Narishige, Japan) with ear bars previously
52 coated with EMLA cream. We monitored anaesthetic depth by checking spinal reflexes and breathing
53 rates. Body temperature was maintained at 37°C using a homeothermic heating pad. Eyes were
54 treated with ophthalmic gel (Viscotears Liquid Gel, Novartis, Switzerland) and the entire scalp was
55 washed with povidone-iodine solution. An area of skin was removed (an oval of 15 mm x 10 mm in
56 the sagittal plane) such that all skull landmarks were visible and sufficient skull was accessible to
57 securely fix a titanium or stainless steel head bar. The exposed periosteum was removed and the bone
58 was washed using saline solution. The bone was dried and then scraped using a scalpel blade to aid
59 bonding of glue. Cyanoacrylic glue (Vetbond, 3M, USA) was applied to bind skin edges to the skull and
60 as a thin layer across the exposed skull to aid bonding to the dental acrylic. A custom titanium or
61 stainless steel head bar (dimensions 22.3 x 3.2 x 1.3 mm; design by Karel Svoboda, Janelia Farm
62 Research Campus, Howard Hughes Medical Institute) [18] was placed directly onto the wet glue
63 centred just posterior to lambda. Once dry, we fixed the head bar firmly in place by applying dental
64 acrylic (Lang Dental, USA) to the head bar (on top and behind) and the skull (anterior). Mice were
65 given buprenorphine (0.5 mg/kg, I.P.) and further EMLA cream to the paws and ears. Once the acrylic
66 was set, anaesthesia was turned off. Animals were housed individually on a reverse 50:50 light-dark
67 (LD) cycle and allowed to recover for one week post-surgery.

68 Head fixation and water delivery

69 Mice were trained using a shaping procedure to freely enter a head fixation device (Figure 1A). We
70 used two device designs. One design consisted of an acrylic tube (32 mm internal diameter) with its
71 head end cut to enable access to implanted head bars. The tube was placed on Parafilm or a rubber
72 glove and clamped into a v-shape groove. This support acted to stabilise the tube, collect faeces and
73 prevent mice from grasping stimulus apparatus and the lickport. The second design consisted of a
74 platform with a custom-made treadmill on which mice could locomote freely (design by Leopoldo
75 Petreanu, Champalimaud Centre for the Unknown). A mesh was fixed over the treadmill to surround
76 the mouse's body, allowing the animal to feel comfortably enclosed rather than exposed. The ends of
77 the head bars were inserted into grooves on two head fixation clamps and tightened using
78 thumbscrews. The head fixation set-up was adapted from [18, 19].

79 Water was available to mice via a spout made from a blunted gauge 13 syringe needle. Water delivery
80 was controlled via a solenoid valve (LDHA1233215H, The Lee Company, France). The acrylic tube or

81 head bar holder was lined with aluminium foil. Terminals from an A/D input of a signal processor
82 (RP2.1, TDT, USA) were then connected to the water spout and the foil. Tongue contacts with the lick
83 port created brief elevations in voltage consistent with lick durations [20].

84 Water restriction

85 To motivate mice to learn and perform the task we employed a water restriction protocol [18] and
86 made water available as a reward during the task. Mice cope better with water control than food
87 control [21]. Unless rodents are motivated by fluid or food control, they can fail to learn even simple
88 sensory tasks [22] and perform too few daily trials for data collection to be satisfactory. We verified
89 that mice were not motivated by sugary treats alone (Lucozade and chocolate milk). We observed a
90 mild increase in motivation when mice were given sunflower seeds before tasks.

91 Mouse water intake was regulated so that animals were motivated to perform at around 75% success
92 rate for 200 or more trials per session under our conditions (45-55% humidity, 23°C and atmospheric
93 pressure; reverse 50:50 LD cycle), while remaining active and healthy. This was achieved with two
94 different schedules, depending on the institution where the experiment took place. In one schedule
95 (Instituto de Neurociencias), we titrated down water availability to the amount required for mice to
96 maintain >75% of initial body mass in the short term and gradually increase body mass in the long
97 term (0.5 ml daily including experimental water rewards collected during the session, 7 days a week).
98 In the other schedule (University of Sussex), mice were restricted to 50% of their average free water
99 intake but given free access to water for a finite period during the dark phase of their LD cycle. Body
100 weight (mass) was monitored throughout the study, and we measured experimental reward water
101 intake by weighing mice before and after the daily behaviour session together with collected faeces.
102 For both schedules, mice initially lost weight but then gradually increased body mass over the course
103 of the experiment. Sensory discrimination training began after 9 days on water control.

104 Animal handling and training

105 We initiated water control one week after head bar implantation, and began to handle animals daily.
106 On days 1 and 2 animals were introduced to the experimenter. On days 3 and 4 animals were
107 introduced to the head fixation device. On days 5 and 6 mice received water via a syringe only when
108 inside the device (but not head-fixed). On days 7 and 8 animals were given a sunflower seed and after
109 ingestion were head-fixed and given water via a syringe. Animals became accustomed to head fixation
110 and expected to receive water from the spout situated in front of their head. On day 9, under light
111 isoflurane anaesthesia (1-2%) all whiskers apart from C2 were trimmed bilaterally. At least 30 minutes
112 later mice began the task. Mice performed a single daily training session. Animals were trained in the
113 dark; illumination, if necessary, was provided by a red lamp.

114 Stimulus delivery and design

115 Our aim was to develop a task whereby tactile sequences delivered to the animal could only be
116 distinguished by discriminating their temporal patterning. Careful control of stimulation patterns was
117 therefore required. To achieve this we delivered controlled stimuli, which animals needed to sense by
118 operating in a “receptive” mode rather than by active whisking [23]. In this design, whiskers were
119 inserted into a small tube. Stimulus sequences were generated as filtered noise vibrations, such that
120 whisker stimulation was continuous during a trial (Figure 1D). We thus avoided temporally isolated
121 discrete movements that could have initiated whisking or confused the animal as to the start, content
122 and ending of the temporal pattern. Upon head fixation at the start of a session, the left C2 whisker
123 was inserted into a snugly fitting tube (pulled 1 ml plastic syringe) glued to a piezoelectric actuator
124 wafer (PL127.11, Physik Instrumente, Germany). The wafer was mounted vertically and motion was

125 rostrocaudal. In some experiments, a different method to deliver stimuli was required: a metallic 10
126 mm² mesh grid was glued to the end of an actuator to enable multiple whisker stimulation and allow
127 quick transition between experiments, as in [Figure 2B,C](#).

128 Stimulus sequences were constructed in Matlab (Mathworks, USA) and played via a signal processor
129 (RP2.1, TDT, USA) controlled with code custom-written in ActiveX software (TDT). The GO sequence
130 lasted 800 ms and consisted of 8 consecutive “syllables”, where each syllable was a 100 ms segment
131 constructed from white noise with one of 4 amplitude levels ([Figure 1D](#)). We constructed the sequence
132 as follows: (1) we created a 100 ms white noise snippet generated at a sampling rate of 12207 Hz (in
133 Matlab), (2) stitched 8 snippets together, (3) multiplied the resulting chain of repeated white noise
134 snippets by an amplitude modulation envelope, (4) convolved this sequence with a Gaussian
135 waveform (SD 1.64 ms) to implement frequency filtering, and (5) normalised the sequence to match
136 the dynamic range of the piezoelectric actuator. In the resulting GO sequence, constituent syllables
137 differed in amplitude: the pattern of noise amplitude modulation was [3 1 4 2 3 1 4 2], with 1 being
138 the lowest amplitude level and 4 the highest. The NO-GO sequence in the full version of the task
139 contained the exact same syllables but in a scrambled order ([Figure 1D](#)), specifically [3 4 2 1 2 4 3 1].
140 The target and non-target sequences were therefore identical for the initial 100 ms. Further sequences
141 were created to aid learning and to explore the nature of recognition, as detailed in Results.

142 [Task control and analysis](#)

143 We trained mice to respond to the GO sequence by licking a spout to receive a water reward (1-2 μ l).
144 On presentation of the NO-GO sequence mice were trained not to lick ([Figure 1B](#)). The trial began with
145 the ‘stimulation period’ (0.8 s) where the sequence was delivered to the whisker. At the end of the
146 stimulation period followed a ‘response period’ (1.5 s) where mice must lick or refrain depending on
147 the stimulus sequence. Following the GO sequence, if mice licked during the response period (a hit
148 trial) they received a water reward; if they failed to lick (a miss trial) the next trial began as normal.
149 Following a NO-GO sequence, if mice correctly withheld licking during the response period (a correct
150 rejection trial) the next trial began as normal; if they licked (a false alarm trial) the next trial was
151 delayed by 2-5 s. Trial parameters were defined in Matlab using a custom made GUI and then loaded
152 to the RP2.1 signal processor. Trial outcomes were recorded in Matlab using custom-written code.

153 Several related measures can be used to quantify performance, including overall percentage of correct
154 trials, hit rate and false positive rate, and d' [22, 24]. Here we present results mostly as percentage of
155 correct trials measured over a 50-trial sliding window during the course of a session. To calibrate this
156 performance measure in terms of statistical significance level, we shuffled stimulus identity and
157 behavioural response (lick/no lick) on a trial by trial basis for each individual session in a test data set
158 of 104 sessions ($n = 7$ animals; shuffling repeated 10000 times per session). Performing shuffling
159 separately for each session allowed us to control for variations in overall lick rate from animal to
160 animal and during the course of training. For all sessions in the test data set, the probability of
161 achieving 75% correct performance given a random relationship between stimulus and responses was
162 lower than $p = 0.001$; the probability of achieving 70% correct given such a relationship was under $p =$
163 0.015.

164 During training, we routinely varied the proportion of GO and NO-GO trials during a session in order
165 to aid learning and keep animals motivated (e.g. the fraction of GO trials could temporarily increase).
166 This could lead to a misleading value of the performance measure. For example, consider a randomly
167 performing mouse that licked on 90% of trials. In a hypothetical 50 trial period with 40 GO and 10 NO-
168 GO trials, it would reach a 90% hit rate on GO trials and a 90% false alarm rate on NO-GO trials. Overall
169 performance would then be 74% correct ($= 0.8 \times 90\% + 0.2 \times 10\%$), despite the mouse performing at

170 chance with no differentiation between GO and NO-GO stimuli. To correct for this, we rebalanced the
171 percentage correct measure so that GO and NO-GO trials are set to have equal weight. This rebalanced
172 measure reports the above hypothetical example as 50% correct ($= 0.5 \times 90\% + 0.5 \times 10\%$).

173 Human experiments

174 Human experiments were conducted and underwent ethical review at the University of Sussex. In
175 total, 59 participants were recruited and gave informed consent. In the human counterpart of the
176 experimental design, the basic GO and NO-GO stimulus waveforms described above ([Figure 1D](#)) were
177 left unchanged. Further waveforms were added in order to aid and test learning as described in
178 Results. Stimuli were loaded to the RP2.1 signal processor and delivered via a piezoelectric wafer
179 identical to that used for whisker stimulation, but with a plastic plate glued on (polyethylene
180 terephthalate; 20 x 10 x 1 mm). The wafer stimulator assembly was supported by a platform
181 incorporating a cushioned armrest. Participants were asked to place one fingertip lightly on the plate's
182 surface ([Figure 1C](#)). The wafer was placed horizontally and vibrations were vertical. A small box
183 containing a button was placed on the same table as the platform, in a position allowing participants
184 to comfortably press the button with their free hand whenever a target stimulus was felt. GO and NO-
185 GO stimulus trials were randomly interleaved. Experiments were conducted with no explicit
186 instruction as to the identity of the target stimulus; instead, participants were asked to press the
187 button whenever they identified a stimulus that felt familiar, more frequent or "special" than others.
188 Participants had to decide by themselves which stimulus constituted the target. Feedback upon
189 correct trials, provided in the form of a "Correct" sign appearing on a computer screen, was given to
190 a subset of participants to more closely mirror the experimental design used with mice. We compared
191 performance with and without feedback: performance was no higher for the participants trained with
192 feedback, so results were pooled together ($p = 0.99$, Wilcoxon rank sum test, $n = 15$ participants
193 without feedback and $n = 44$ with feedback).

194

195 Results

196 Achieving sequence recognition by mice

197 We sought to train mice to recognise a target stimulation sequence delivered to their whiskers. Our
198 aim was for mice to distinguish the target sequence based on the order in which its elements
199 appeared. To this end, mice were trained to distinguish between initially meaningless GO and NO-GO
200 sequences built from series of identical "syllables", with the sequences differing only in that syllables
201 were scrambled in time over hundreds of milliseconds (each individual syllable lasting 100 ms, for a
202 total of 8 syllables; [Figure 1D](#)). The initial syllable was identical across GO and NO-GO sequences in
203 order to avoid providing a stimulus onset cue ([Figure 1D](#)).

204 Mice ($n = 22$) were trained to associate the GO stimulus with a water reward by making water available
205 when the GO stimulus was delivered; on the first few days of training, no other whisker stimuli were
206 given, so that mice effectively learned to detect whisker stimulation. As soon as animals demonstrated
207 detection (75% correct detection trials), we introduced an initial NO-GO sequence. To make this stage
208 easier, this initial NO-GO sequence consisted of a square wave riding upon low amplitude noise,
209 distinctly different from the GO sequence ([Figure 1D](#)). Mice quickly learned to distinguish the square
210 wave stimulus from the GO waveform (75% correct; within 4 sessions; [Figure 2A](#)). They were
211 immediately moved to the next stage of training to avoid creating an artefactual generalized
212 association between "noisy" stimuli (as opposed to square waves) and water availability. In the

213 following —more demanding— stage, the NO-GO sequence consisted of a scrambled GO sequence
214 with half (4 of 8) syllables knocked out (Figure 1D).

215 Mice accomplished each stage of training within a few days (Figure 2A), performing approximately
216 200-300 trials per daily session (mean 249 trials; SD 71 trials; total n = 456 sessions in 22 mice). During
217 this process, recognition of the GO sequence was mediated by the animal's whiskers: performance
218 fell to chance level upon removing the whiskers from the moving stimulator (Figure 2B). Performance
219 recognising the GO sequence was robust against variations in how the sequence was presented: daily
220 changes in the tube's positioning relative to the stimulated whisker did not noticeably affect
221 performance. To test this invariance more specifically, in a subset of experiments mice were trained
222 on a multi-whisker version of the task where whiskers (left untrimmed) were inserted into a wire mesh
223 attached to the piezo actuator. Whiskers were first removed from the stimulator mesh; then, after a
224 period of trials with stimulator movement but no whisker stimulation —during which performance
225 dropped to chance level—, the actuator was rotated 90° and whiskers reinserted into the mesh.
226 Reinsertion and stimulator rotation changed the identity and set-point of whiskers being stimulated
227 as well as the direction of stimulation. Yet performance recovered to the level reached before whisker
228 removal (Figure 2C; repeated for n = 4 mice; p = 0.44; Wilcoxon signed rank test). Sequence recognition
229 therefore transferred across different stimulation configurations.

230 In the final stage of training, the NO-GO sequence comprised identical syllables to the full GO sequence
231 but scrambled in time: that is, syllable ordering changed (Figure 1D). Mice that underwent training up
232 to this final stage performed beyond 70% on at least one session (mean 72.8%, SD 9.4%; n = 5 out of
233 6 mice). Animals could maintain their performance over several days, albeit with fluctuations (Figure
234 2G), again despite day-to-day variability in how the whisker was attached to the stimulator. On every
235 stage of training, improvements in performance occurred mainly through learning to withhold
236 impulsive false alarm responses (licks) (Figure 2D-F,H), in common with other discrimination tasks in
237 mice [18, 25]. Thus, high performance was associated with low false alarm rates (Figure 2H). These
238 experiments show that mice learned to distinguish whisker-mediated stimuli that differed from others
239 only in their temporal patterning over hundreds of milliseconds.

240 Rapid learning of noisy sequences by humans

241 We tested whether humans could also learn to recognise the same temporally patterned tactile noise
242 stimuli, delivering the patterns through an actuator applied to a fingertip. Participants were asked to
243 indicate recognition of the target sequence by pressing a button. They first underwent a training
244 session in which the GO target sequence was interleaved with a series of non-target stimuli. Early in
245 the session, the non-target patterns were easily distinguishable from the GO pattern; later, these
246 clearly distinct patterns were replaced by NO-GO sequences that differed from the GO target only in
247 that their constituent syllables were scrambled, as in the final stage of mouse training. Human
248 participants quickly improved their performance over the course of this session, typically converging
249 to a steady level of performance despite the increase in difficulty during the session (Figure 3A). This
250 indicated fast learning of the GO sequence. Performance as tested after the end of this learning phase
251 was maintained in a later session separated by at least one week, suggesting remarkable robustness
252 (Figure 3B; retest performance was actually higher, although the difference did not reach significance;
253 p = 0.0547; n = 11 participants; Wilcoxon signed rank test).

254 Potential cues for sequence recognition: binary sequences

255 Which cues are robust correlates of sequence identity, and which can be used by an animal? In our
256 task, possible cues could range across timescales from global to local, as follows (Figure 4A). At the

257 highest (most global) level the GO sequence could be recognised by extracting its overall ordering rule
258 ([3 1 4 2 3 1 4 2] versus other scrambled orders). However, recognition could also stem from detection
259 of specific syllables. For example, in the GO sequence [3 1 4 2 3 1 4 2] the second 100 ms syllable was
260 smaller in magnitude than the first, in contrast to the NO-GO sequence [3 4 2 1 2 4 3 1], whose second
261 syllable was greater than the first (Figure 1D). Thus, detecting a downwards modulation in noise
262 amplitude after 100 ms could enable recognition. Potentially, a more local strategy based on detecting
263 even briefer, sub-syllabic events or “landmarks” in the sequence, such as fluctuations in whisker
264 velocity happening in a certain relative order (Figure 4A), could also be possible. We wondered which
265 strategies were accessible to mice and humans.

266 First, any overall temporal average or summation of stimulus parameters throughout the duration of
267 the sequence could be ruled out as a cue, because GO and NO-GO sequences consisted of identical,
268 but scrambled elements. Moreover, animals often started licking on GO trials before the end of
269 sequence presentation (Figure 2D-F), suggesting that just a few transitions in noise modulation or
270 stimulus landmarks sufficed for the animal to reach its decision as to sequence identity.

271 To begin to explore the ability of mice to exploit specific cues for sequence recognition, we designed
272 a version of the task in which the GO target sequence consisted of a simple succession of epochs of
273 large and small noise amplitude: using the same notation as above, [4 1 4 1 1 1 4 1] (Figure 4B). A
274 separate set of animals (n = 10) was trained to distinguish this new GO sequence from a NO-GO
275 sequence that, as before, differed only in its temporal patterning: [4 1 1 1 4 1 4 1] (Figure 4B). These
276 sequences were simpler than the original design in that they were binary: their constituent syllables
277 were only “large” (4) or “small” (1). These simpler temporal patterns were potentially distinguishable
278 based on syllable ordering or on the different durations of small-amplitude epochs: for example, in
279 the binary GO target sequence the first “small” epoch lasted just 100 ms, but in the NO-GO it lasted
280 for a total of 300 ms (because comprising three syllables). Yet mice performed poorly at distinguishing
281 [4 1 4 1 1 1 4 1] from [4 1 1 1 4 1 4 1] (Figure 4C; n = 3) despite having been trained exclusively on this
282 variant of the task. In particular, animals consistently displayed high false alarm rates, suggesting that
283 they failed to detect what made the binary NO-GO stimulus different from the binary GO (data not
284 shown). This suggested that mice either did not detect the simpler, binary stimulus modulation epochs
285 or did not recognise their differential duration.

286 To distinguish between these possibilities, we tested performance on probe sessions with two variants
287 of the binary NO-GO sequence. In the first variation, the binary GO target remained identical as [4 1 4
288 1 1 1 4 1], but the NO-GO sequence was [4 1 1 1 1 1 4 4]. This alternative NO-GO stimulus had the
289 same number of large and small syllables as the one in the previous paragraph, but a different
290 temporal arrangement, with all small-amplitude syllables appearing consecutively and forming a
291 single very long central period (Figure 4B). The sequence therefore effectively had just two “large”
292 epochs, at the beginning and at the end, and a single very long “small” epoch. It was therefore
293 expected to be easier to discriminate from the GO sequence despite having the same overall energy.
294 In the second variation, the binary GO target also remained identical and the NO-GO stimulus was [4
295 1 1 1 1 1 1 1] (Figure 4B). The goal of this variation was to check whether mice could straightforwardly
296 distinguish large or small syllables. In both of these variants animals performed better than in the
297 original binary design (Figure 4C; $p < 10^{-9}$; n = 7 mice and n = 161 sessions; generalised linear mixed-
298 effects model). Note that performance in the simpler variants was at a level comparable to that of the
299 original GO vs NO-GO paradigm (Figure 4C). Mice also successfully distinguished the binary GO
300 sequence from noise stimuli with no modulation, i.e. with constant noise amplitude: [1 1 1 1 1 1 1 1]
301 or [2 2 2 2 2 2 2 2] (percentage correct > 75% for all animals for [1 1 1 1 1 1 1 1], 3 out of 4 for [2 2 2 2
302 2 2 2]; n = 4 mice; data not shown). The overall conclusion of the binary sequence experiments is that

303 mice could detect “large” epochs and recognise their number, and use the presence of relative
304 modulations in noise amplitude as cues, but could not as readily use the duration of each modulation
305 epoch.

306 In contrast to mice, humans rapidly performed well on the [4 1 4 1 1 1 4 1] vs [4 1 1 1 4 1 4 1] version
307 of the task (Figure 4C), even when they had had no prior exposure to the version in Figure 3 (5 out of
308 8 participants). They achieved high performance within one training session. They also subjectively
309 reported being able to use the relative durations of “small” and “large” epochs as a cue. Thus, humans
310 appeared to have access to more cues for sequence discrimination than mice, including the duration
311 and ordering of intervals in noise modulation.

312 Potential cues for sequence recognition: fixed landmarks

313 Our findings suggested that humans could discriminate sequences based on multiple cues. We
314 wondered whether, in addition to being sensitive to the size and timing of noise amplitude
315 modulations, human participants might also rely on detecting learned sub-syllabic “landmarks”, i.e.
316 specific brief events or fluctuations within the stimulus waveform (Figure 4A). To address this, we
317 assessed whether the presence of fixed waveforms influenced performance.

318 Upon training participants on the initial version of the task (Figure 3), we tested performance on a
319 variant of the design with two types of GO trials. The first type of trial used a target sequence
320 constructed by applying amplitude modulation to a waveform that was identical (repeated) across
321 syllables and trials (“frozen”). This sequence was used throughout training and in the experiments of
322 Figures 1-3. The second type of trial presented a sequence built by modulating a noise waveform that
323 varied on every repeat (“unfrozen”) (Figure 4D). For unfrozen sequences, each of the 8 syllables was
324 based on a different noise snippet and each trial was constructed from a fresh waveform. Thus, in this
325 type of trial, the amplitude modulation envelope characteristic of the GO sequence remained identical
326 across target trials, but not the precise stimulus values, so that sub-syllabic fluctuations were not
327 conserved. Frozen and unfrozen GO trials were interleaved within a session. Note that unfrozen
328 waveforms could vary in their empirical standard deviation, potentially leading to a confound caused
329 by variability in perceived stimulus amplitude. To control for this, we included in our analysis only
330 stimuli matched for empirical standard deviation. We compared hit rates for both types of GO trial
331 (Figure 4E). Hit rates varied little across type of trial (frozen trials mean 0.76, SD 0.17; unfrozen trials
332 mean 0.73, SD 0.19; $p = 0.09$; $n = 27$ participants; Wilcoxon signed rank test). Thus, participants did
333 not require specific brief waveform landmarks to achieve sequence recognition.

334 In conclusion, humans could use cues based on ordering, timing and feature detection to recognise a
335 target tactile temporal sequence. Mice tested with an identical stimulus paradigm also achieved
336 recognition of a sequence delivered to their whiskers, but appeared to base their performance
337 primarily on the presence of particular relative changes in noise amplitude.

338

339 Discussion

340 Senses such as touch or hearing depend critically on the detection of temporal patterning over
341 timescales from tens of milliseconds to seconds: in these sensory modalities, signals unfold over time
342 and are incomprehensible if the temporal relationship between their elements is lost. Sequence
343 learning and the processing of temporal duration are impaired in psychiatric disorders including
344 depression and schizophrenia (e.g. [26-29]). Here, we developed an assay suitable for evaluating
345 tactile sequence discrimination. Mice learned to distinguish a target stimulation sequence delivered

346 to their whiskers: the sequence differed from others only in its temporal ordering over hundreds of
347 milliseconds. Humans receiving identical sequential stimuli applied to their fingertip also rapidly
348 learned to perform the task.

349 Similar human paradigms have been used to discover implicit learning of meaningless auditory noise
350 patterns [30], demonstrating that patterned noise learning generalises across species and sensory
351 systems. In rodents, our design provides an assay for elucidating how neurons within sensory circuits
352 respond and interact under temporally patterned stimulation.

353 Mechanisms for memorising and determining sequence identity regardless of syntax and semantics
354 have been proposed to be precursors to speech recognition [1, 31, 32]. In our paradigm, sequences
355 were built from chunks of noise with no semantic content or prior meaning. Structural rules such as
356 those aiding interpretation of music or speech (grammar, syntax) were not present as cues. The
357 protocol involved learning only a single instance of a GO target sequence, and did not test
358 generalisation and rule abstraction. However, it would be straightforward to modify the present
359 design to one whereby decisions need to be made based on sequencing or branching rules.

360 Sequential transitions in texture may be encountered by mice running along walls or tunnels [33, 34]
361 and “receptive” sensation is also routinely mediated by whiskers [23]. Our principal aim in this study
362 was to identify behavioural capacities for learning and recognition of tactile temporal sequences and
363 lay the ground for exploring whether these generalise across domains. A classical approach in
364 comparative cognition employs tasks that are not part of an animal’s natural repertoire to challenge
365 its capacities [35-39].

366 Although mice and humans were both able to learn to recognise a sequence identifiable by the order
367 of its elements, humans appeared to be capable of accessing a wider range of cues than mice. It is
368 difficult to separate this result from the obvious differences in our ability to communicate task
369 parameters to humans and mice. Our results suggest that mice relied primarily on particular relative
370 fluctuations in stimulus attributes (kinetic or kinematic) over time. Mice could detect “large
371 amplitude” epochs and recognise their number, and could therefore use relative modulations in noise
372 amplitude as cues. In the experiment shown in [Figure 2](#), mice often began licking before the end of
373 the GO target sequence ([Figure 2D,F](#)), suggesting that they may have identified the target by detecting
374 particular changes in noise amplitude occurring relatively early in the sequence. In the experiment in
375 [Figure 4](#), mice could not distinguish the GO sequence from others with the same number of “large”
376 and “small” epochs. They did successfully recognise the GO sequence compared to stimuli where the
377 noise amplitude remained constant, regardless of whether the integrated energy of those stimuli
378 matched or exceeded that of the GO sequence, and with no need for prior training (data not shown).
379 This implies that animals used sensitivity to relative changes in noise amplitude as a behavioural cue,
380 a capacity previously demonstrated in rats under a more cognitively demanding task design [40].
381 Further testing of mouse capacities for abstracting sequencing rules is needed.

382 Humans appeared to use global and local information on fluctuations in stimulus amplitude to arrive
383 at a heuristic for sequence recognition. Participants receiving the GO sequence often reported feeling
384 a distinct buzzing vibration or counting “beats” in the stimulus, but reported no explicit awareness of
385 a change in sequence element ordering. In a previous auditory study, human listeners were asked to
386 report when a noise stimulus consisted of concatenated repeats of an identical 500 ms segment as
387 opposed to a single 1 s segment [30]. Listeners improved their ability to detect the repeated-noise
388 stimuli when they were unwittingly exposed to the stimulus a few times, and this improvement in
389 performance seemed related to the learning and detection of low-level stimulus waveform features
390 (i.e. particular structures appearing in the noise) [30, 41]. It is likely that the presence of certain

391 learned features, appearing with a specific temporal relationship to each other, provides an
392 elementary cue for discriminating and recognising sequences on timescales of hundreds of
393 milliseconds to seconds across modalities. Determining the duration of the relevant features and how
394 they are encoded [42-44] is a further important task.

395 Future work must examine how neuronal circuits detect and recognise temporally patterned
396 stimulation sequences. Neurons in early stages of sensory pathways transform any temporally
397 patterned sensory signal into a sequence of precisely timed spikes, so recognising a sensory stimulus
398 with a characteristic temporal pattern –e.g., to discriminate one tactile texture from another [14]–
399 ultimately implies a need for circuits in higher brain areas to decode a spatiotemporal spike sequence.
400 For the paradigm explored here, this capacity is likely to reside within the neocortex, as suggested by
401 the following findings. In the rodent whisker system, neurons in subcortical stages and primary
402 somatosensory cortex display limited temporal integration [45-51]. Therefore, integration over time
403 to represent specific whisker stimulation sequences must be carried out by higher cortical circuits [50-
404 53]. That mice were able to generalise the task across different whisker stimulation directions ([Figure](#)
405 [2C](#)), which would have evoked responses in different subsets of neurons at each stage in the pathway
406 [54], suggests further evidence for higher cortical task involvement. A hierarchical scheme whereby
407 later stages of cortical processing can integrate stimuli over longer timescales is consistent with
408 findings in primates [55, 56].

409 Which mechanisms contribute to setting integration timescales? Single neurons can be sensitive to
410 spatiotemporal input sequences [57-59]. Learning to detect a specific sequence [60] can be
411 accomplished by spike timing-dependent plasticity [61-63]. Timescales for integration of sequences
412 could be regulated by activation of local inhibition [64]. Sequence-selective responses can emerge as
413 a result of sensory exposure to the target [65]. Finally, heterogeneous timescales for integration across
414 cortical processing stages may arise from differences in large-scale connectivity across areas [66, 67].
415 It remains to be determined how these and other mechanisms come together to implement sequence
416 recognition in cortical circuits in vivo.

417

418 Acknowledgments

419 This work was supported by the Spanish Ministry of Science and Innovation (grant number BFU2011-
420 23049, co-funded by the European Regional Development Fund; Subprograma Ayudas FPI-MICINN,
421 BES-2012-052293), the Medical Research Council (grant number MR/P006639/1), the Valencia
422 Regional Government (ACOMP2010/199 and PROMETEO/2011/086), and the University of Sussex
423 internal research development fund. The authors declare no competing financial interests.

424 We thank Karel Svoboda for sharing designs, advice and equipment, Leopoldo Petreanu for sharing
425 designs, Rasmus Petersen for sharing code for behaviour control and for comments on an earlier
426 version of the manuscript, and Elena Giusto for technical help and for the drawings in Figure 1.

427

428 References

- 429 1. Wilson, B., Marslen-Wilson, W.D., and Petkov, C.I. (2017). Conserved Sequence Processing in
430 Primate Frontal Cortex. *Trends Neurosci* *40*, 72-82.
- 431 2. Lashley, K.S. (1951). The problem of serial order in behavior. In *Cerebral Mechanisms in*
432 *Behavior: The Hixon Symposium*, L.A. Jeffress, ed. (New York, NY: John Wiley), pp. 112-146.

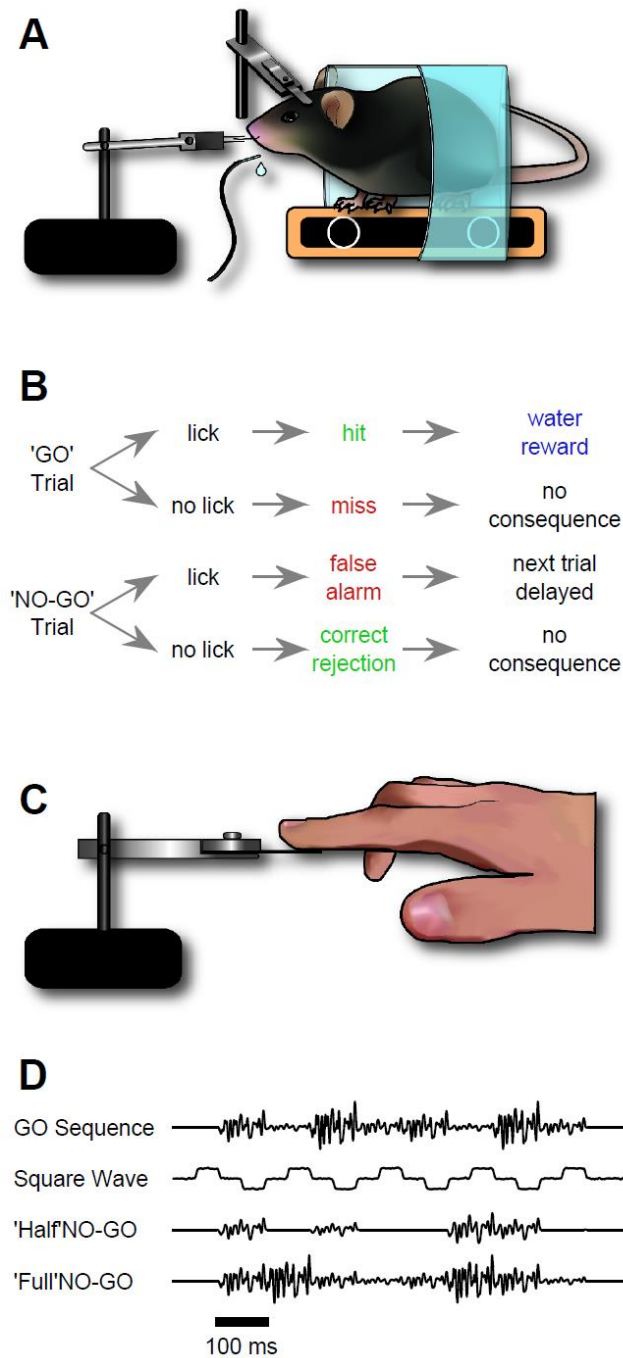
- 433 3. Griffiths, T.D., and Warren, J.D. (2004). What is an auditory object? *Nat Rev Neurosci* 5, 887-
434 892.
- 435 4. Dehaene, S., Meyniel, F., Wacongne, C., Wang, L., and Pallier, C. (2015). The Neural
436 Representation of Sequences: From Transition Probabilities to Algebraic Patterns and
437 Linguistic Trees. *Neuron* 88, 2-19.
- 438 5. Johnson, K.O. (2001). The roles and functions of cutaneous mechanoreceptors. *Curr Opin*
439 *Neurobiol* 11, 455-461.
- 440 6. Johansson, R.S., and Birznieks, I. (2004). First spikes in ensembles of human tactile afferents
441 code complex spatial fingertip events. *Nat Neurosci* 7, 170-177.
- 442 7. Bale, M.R., Campagner, D., Erskine, A., and Petersen, R.S. (2015). Microsecond-scale timing
443 precision in rodent trigeminal primary afferents. *J Neurosci* 35, 5935-5940.
- 444 8. Chagas, A.M., Theis, L., Sengupta, B., Stuttgen, M.C., Bethge, M., and Schwarz, C. (2013).
445 Functional analysis of ultra high information rates conveyed by rat vibrissal primary
446 afferents. *Front Neural Circuits* 7, 190.
- 447 9. Jones, L.M., Lee, S., Trageser, J.C., Simons, D.J., and Keller, A. (2004). Precise temporal
448 responses in whisker trigeminal neurons. *J Neurophysiol* 92, 665-668.
- 449 10. Campagner, D., Evans, M.H., Bale, M.R., Erskine, A., and Petersen, R.S. (2016). Prediction of
450 primary somatosensory neuron activity during active tactile exploration. *Elife* 5.
- 451 11. Bush, N.E., Schroeder, C.L., Hobbs, J.A., Yang, A.E., Huet, L.A., Solla, S.A., and Hartmann, M.J.
452 (2016). Decoupling kinematics and mechanics reveals coding properties of trigeminal
453 ganglion neurons in the rat vibrissal system. *Elife* 5.
- 454 12. Phillips, J.R., and Johnson, K.O. (1985). Neural mechanisms of scanned and stationary touch.
455 *The Journal of the Acoustical Society of America* 77, 220-224.
- 456 13. Phillips, J.R., Johansson, R.S., and Johnson, K.O. (1990). Representation of braille characters
457 in human nerve fibres. *Exp Brain Res* 81, 589-592.
- 458 14. Weber, A.I., Saal, H.P., Lieber, J.D., Cheng, J.W., Manfredi, L.R., Dammann, J.F., 3rd, and
459 Bensmaia, S.J. (2013). Spatial and temporal codes mediate the tactile perception of natural
460 textures. *Proc Natl Acad Sci U S A* 110, 17107-17112.
- 461 15. Saal, H.P., Wang, X., and Bensmaia, S.J. (2016). Importance of spike timing in touch: an
462 analogy with hearing? *Curr Opin Neurobiol* 40, 142-149.
- 463 16. Maravall, M., and Diamond, M.E. (2014). Algorithms of whisker-mediated touch perception.
464 *Curr Opin Neurobiol* 25, 176-186.
- 465 17. Sofroniew, N.J., and Svoboda, K. (2015). Whisking. *Curr Biol* 25, R137-140.
- 466 18. Guo, Z.V., Hires, S.A., Li, N., O'Connor, D.H., Komiyama, T., Ophir, E., Huber, D., Bonardi, C.,
467 Morandell, K., Gutnisky, D., et al. (2014). Procedures for behavioral experiments in head-
468 fixed mice. *PLoS One* 9, e88678.
- 469 19. O'Connor, D.H., Clack, N.G., Huber, D., Komiyama, T., Myers, E.W., and Svoboda, K. (2010).
470 Vibrissa-based object localization in head-fixed mice. *J Neurosci* 30, 1947-1967.
- 471 20. Hayar, A., Bryant, J.L., Boughter, J.D., and Heck, D.H. (2006). A low-cost solution to measure
472 mouse licking in an electrophysiological setup with a standard analog-to-digital converter. *J*
473 *Neurosci Methods* 153, 203-207.
- 474 21. Tucci, V., Hardy, A., and Nolan, P.M. (2006). A comparison of physiological and behavioural
475 parameters in C57BL/6J mice undergoing food or water restriction regimes. *Behav Brain Res*
476 173, 22-29.
- 477 22. Carandini, M., and Churchland, A.K. (2013). Probing perceptual decisions in rodents. *Nat*
478 *Neurosci* 16, 824-831.
- 479 23. Diamond, M.E., and Arabzadeh, E. (2013). Whisker sensory system - from receptor to
480 decision. *Prog Neurobiol* 103, 28-40.
- 481 24. Green, D.M., and Swets, J.A. (1966). *Signal Detection Theory and Psychophysics*, (New York:
482 Wiley).

- 483 25. Berdichevskaia, A., Caze, R.D., and Schultz, S.R. (2016). Performance in a GO/NOGO
484 perceptual task reflects a balance between impulsive and instrumental components of
485 behaviour. *Sci Rep* 6, 27389.
- 486 26. Fischer, F. (1929). Zeitstruktur und Schizophrenie. *Zeitschrift für die gesamte Neurologie und*
487 *Psychiatrie* 121, 544-574.
- 488 27. Marvel, C.L., Schwartz, B.L., Howard, D.V., and Howard, J.H., Jr. (2005). Implicit learning of
489 non-spatial sequences in schizophrenia. *J Int Neuropsychol Soc* 11, 659-667.
- 490 28. Siegert, R.J., Weatherall, M., and Bell, E.M. (2008). Is implicit sequence learning impaired in
491 schizophrenia? A meta-analysis. *Brain Cogn* 67, 351-359.
- 492 29. Abrahamse, E.L., van der Lubbe, R.H., and Verwey, W.B. (2009). Sensory information in
493 perceptual-motor sequence learning: visual and/or tactile stimuli. *Exp Brain Res* 197, 175-
494 183.
- 495 30. Agus, T.R., Thorpe, S.J., and Pressnitzer, D. (2010). Rapid formation of robust auditory
496 memories: insights from noise. *Neuron* 66, 610-618.
- 497 31. Petkov, C.I., and Jarvis, E.D. (2012). Birds, primates, and spoken language origins: behavioral
498 phenotypes and neurobiological substrates. *Front Evol Neurosci* 4, 12.
- 499 32. Comins, J.A., and Gentner, T.Q. (2014). Temporal pattern processing in songbirds. *Curr Opin*
500 *Neurobiol* 28, 179-187.
- 501 33. Jenks, R.A., Vaziri, A., Boloori, A.R., and Stanley, G.B. (2010). Self-motion and the shaping of
502 sensory signals. *J Neurophysiol* 103, 2195-2207.
- 503 34. Sofroniew, N.J., Cohen, J.D., Lee, A.K., and Svoboda, K. (2014). Natural whisker-guided
504 behavior by head-fixed mice in tactile virtual reality. *J Neurosci* 34, 9537-9550.
- 505 35. Gould, J.L. (2004). Animal cognition. *Curr Biol* 14, R372-375.
- 506 36. Roth, G., and Dicke, U. (2005). Evolution of the brain and intelligence. *Trends Cogn Sci* 9,
507 250-257.
- 508 37. Alem, S., Perry, C.J., Zhu, X., Loukola, O.J., Ingraham, T., Sovik, E., and Chittka, L. (2016).
509 Associative Mechanisms Allow for Social Learning and Cultural Transmission of String Pulling
510 in an Insect. *PLoS Biol* 14, e1002564.
- 511 38. Loukola, O.J., Perry, C.J., Coscos, L., and Chittka, L. (2017). Bumblebees show cognitive
512 flexibility by improving on an observed complex behavior. *Science* 355, 833-836.
- 513 39. Ishiyama, S., and Brecht, M. (2016). Neural correlates of ticklishness in the rat
514 somatosensory cortex. *Science* 354, 757-760.
- 515 40. Fassihi, A., Akrami, A., Esmaeili, V., and Diamond, M.E. (2014). Tactile perception and
516 working memory in rats and humans. *Proc Natl Acad Sci U S A* 111, 2331-2336.
- 517 41. Andrillon, T., Kouider, S., Agus, T., and Pressnitzer, D. (2015). Perceptual learning of acoustic
518 noise generates memory-evoked potentials. *Curr Biol* 25, 2823-2829.
- 519 42. Jadhav, S.P., Wolfe, J., and Feldman, D.E. (2009). Sparse temporal coding of elementary
520 tactile features during active whisker sensation. *Nat Neurosci* 12, 792-800.
- 521 43. Waiblinger, C., Brugger, D., and Schwarz, C. (2015). Vibrotactile discrimination in the rat
522 whisker system is based on neuronal coding of instantaneous kinematic cues. *Cereb Cortex*
523 25, 1093-1106.
- 524 44. Waiblinger, C., Brugger, D., Whitmire, C.J., Stanley, G.B., and Schwarz, C. (2015). Support for
525 the slip hypothesis from whisker-related tactile perception of rats in a noisy environment.
526 *Front Integr Neurosci* 9, 53.
- 527 45. Maravall, M., Petersen, R.S., Fairhall, A.L., Arabzadeh, E., and Diamond, M.E. (2007). Shifts in
528 coding properties and maintenance of information transmission during adaptation in barrel
529 cortex. *PLoS Biol* 5, e19.
- 530 46. Jacob, V., Le Cam, J., Ego-Stengel, V., and Shulz, D.E. (2008). Emergent properties of tactile
531 scenes selectively activate barrel cortex neurons. *Neuron* 60, 1112-1125.

- 532 47. Petersen, R.S., Brambilla, M., Bale, M.R., Alenda, A., Panzeri, S., Montemurro, M.A., and
533 Maravall, M. (2008). Diverse and temporally precise kinetic feature selectivity in the VPM
534 thalamic nucleus. *Neuron* 60, 890-903.
- 535 48. Stuttgen, M.C., and Schwarz, C. (2010). Integration of vibrotactile signals for whisker-related
536 perception in rats is governed by short time constants: comparison of neurometric and
537 psychometric detection performance. *J Neurosci* 30, 2060-2069.
- 538 49. Estebanez, L., El Boustani, S., Destexhe, A., and Shulz, D.E. (2012). Correlated input reveals
539 coexisting coding schemes in a sensory cortex. *Nat Neurosci* 15, 1691-1699.
- 540 50. Pitas, A., Albarracin, A.L., Molano-Mazon, M., and Maravall, M. (2016). Variable Temporal
541 Integration of Stimulus Patterns in the Mouse Barrel Cortex. *Cereb Cortex*.
- 542 51. McGuire, L.M., Telian, G., Laboy-Juarez, K.J., Miyashita, T., Lee, D.J., Smith, K.A., and
543 Feldman, D.E. (2016). Short Time-Scale Sensory Coding in S1 during Discrimination of
544 Whisker Vibrotactile Sequences. *PLoS Biol* 14, e1002549.
- 545 52. Lim, Y., Lagoy, R., Shinn-Cunningham, B.G., and Gardner, T.J. (2016). Transformation of
546 temporal sequences in the zebra finch auditory system. *Elife* 5.
- 547 53. Fassihi, A., Akrami, A., Schönfelder, V.H., and Diamond, M.E. (2015). Temporal integration in
548 a vibrotactile delayed comparison task: From sensory coding to decision in humans and rats.
549 In *Society for Neuroscience Meeting*. (Chicago, IL).
- 550 54. Bale, M.R., and Petersen, R.S. (2009). Transformation in the neural code for whisker
551 deflection direction along the lemniscal pathway. *J Neurophysiol* 102, 2771-2780.
- 552 55. Hasson, U., Yang, E., Vallines, I., Heeger, D.J., and Rubin, N. (2008). A hierarchy of temporal
553 receptive windows in human cortex. *J Neurosci* 28, 2539-2550.
- 554 56. Honey, C.J., Thesen, T., Donner, T.H., Silbert, L.J., Carlson, C.E., Devinsky, O., Doyle, W.K.,
555 Rubin, N., Heeger, D.J., and Hasson, U. (2012). Slow cortical dynamics and the accumulation
556 of information over long timescales. *Neuron* 76, 423-434.
- 557 57. Segundo, J.P., Moore, G.P., Stensaas, L.J., and Bullock, T.H. (1963). Sensitivity of Neurones in
558 *Aplysia* to Temporal Pattern of Arriving Impulses. *The Journal of experimental biology* 40,
559 643-667.
- 560 58. Branco, T., Clark, B.A., and Hausser, M. (2010). Dendritic discrimination of temporal input
561 sequences in cortical neurons. *Science* 329, 1671-1675.
- 562 59. Baker, C.A., Ma, L., Casareale, C.R., and Carlson, B.A. (2016). Behavioral and Single-Neuron
563 Sensitivity to Millisecond Variations in Temporally Patterned Communication Signals. *J*
564 *Neurosci* 36, 8985-9000.
- 565 60. Hardy, N.F., and Buonomano, D.V. (2016). Neurocomputational Models of Interval and
566 Pattern Timing. *Curr Opin Behav Sci* 8, 250-257.
- 567 61. Masquelier, T., Guyonneau, R., and Thorpe, S.J. (2008). Spike timing dependent plasticity
568 finds the start of repeating patterns in continuous spike trains. *PLoS One* 3, e1377.
- 569 62. Klampfl, S., and Maass, W. (2013). Emergence of dynamic memory traces in cortical
570 microcircuit models through STDP. *J Neurosci* 33, 11515-11529.
- 571 63. Gütig, R. (2014). To spike, or when to spike? *Curr Opin Neurobiol* 25, 134-139.
- 572 64. Kepecs, A., and Fishell, G. (2014). Interneuron cell types are fit to function. *Nature* 505, 318-
573 326.
- 574 65. Gavornik, J.P., and Bear, M.F. (2014). Learned spatiotemporal sequence recognition and
575 prediction in primary visual cortex. *Nat Neurosci* 17, 732-737.
- 576 66. Chaudhuri, R., Bernacchia, A., and Wang, X.J. (2014). A diversity of localized timescales in
577 network activity. *Elife* 3, e01239.
- 578 67. Chaudhuri, R., Knoblauch, K., Gariel, M.A., Kennedy, H., and Wang, X.J. (2015). A Large-Scale
579 Circuit Mechanism for Hierarchical Dynamical Processing in the Primate Cortex. *Neuron* 88,
580 419-431.

581

582 **Figures**



583

584 **Figure 1. Design of sequence recognition task for mice and humans.**

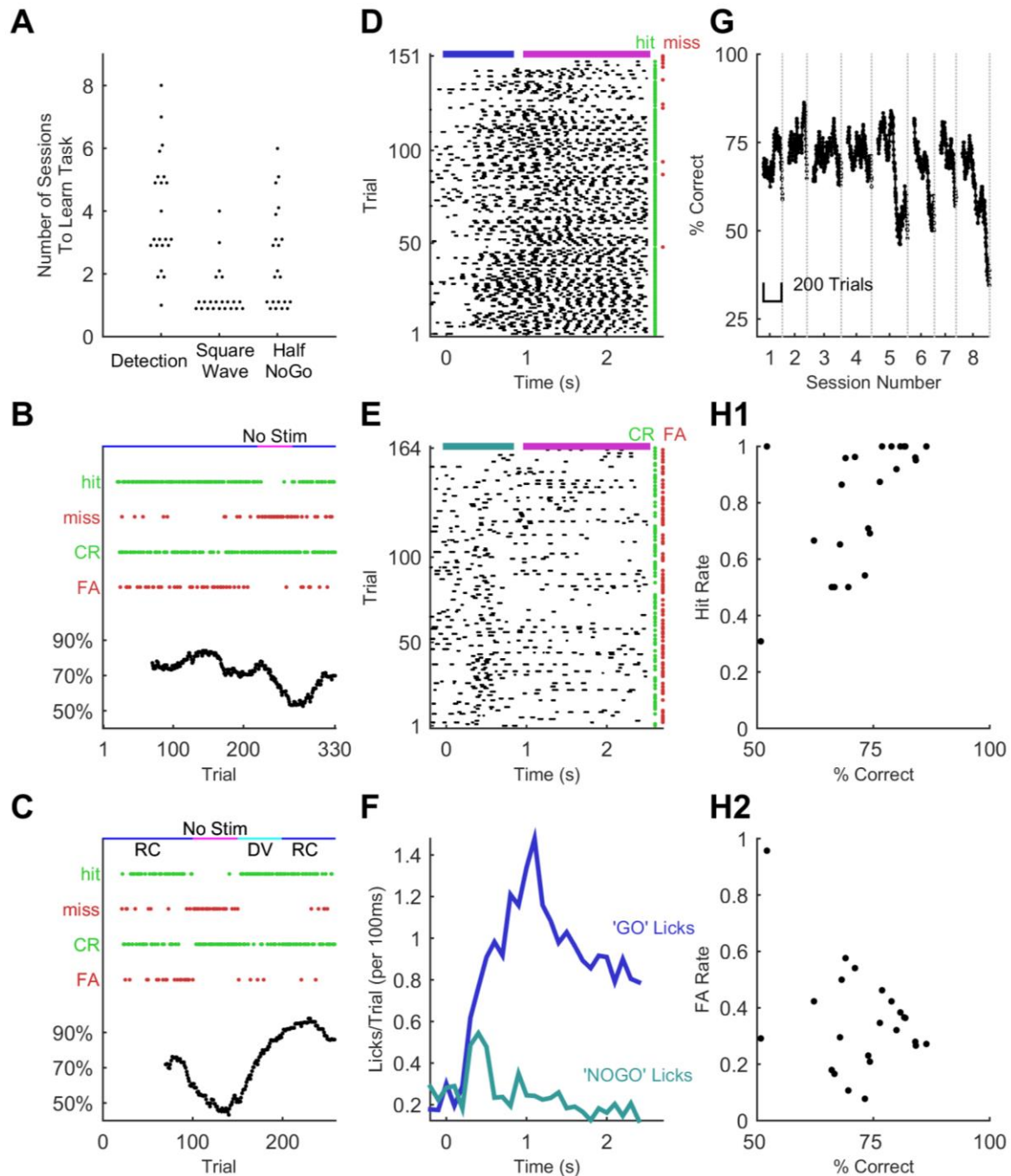
585 A. Illustration of the treadmill-based behavioural and stimulus delivery setup for head-fixed mice.

586 B. Block diagram representing the structure of the GO/NO-GO paradigm. On GO trials, a mouse
587 licking the water spout within the response period (hit) was rewarded with a water droplet. If the
588 mouse licked on a NO-GO trial (false alarm), the next trial was delayed by 2-5 s.

589 C. Illustration of the stimulus delivery setup for human experiments.

590 D. Stimulus sequences for discrimination and intermediate 'shaping' sequences.

591



592

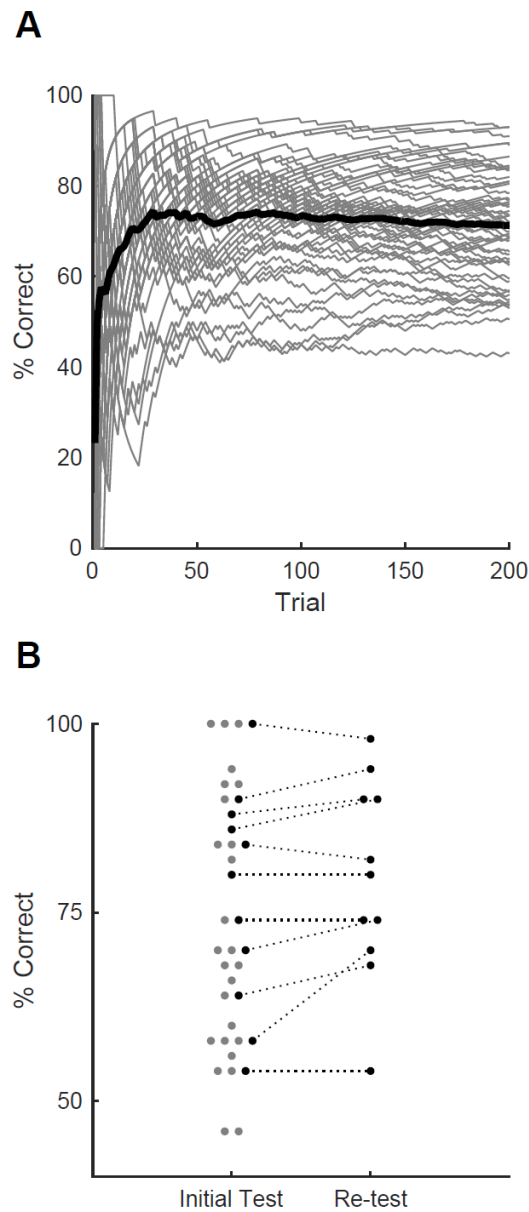
593 **Figure 2. Sequence learning performance in mice.**

594 A. Number of training sessions needed to learn different training stages (75% performance criterion).
 595 Each dot, one mouse. Dots are jittered for visualisation.

596 B. Performance metrics for an example training session (discrimination of the GO sequence from
 597 square wave). Correct trials are green dots, incorrect are red dots. Performance quantified as %
 598 correct over a 50-trial moving window (bottom). Whisker dependency on the task was verified by
 599 removing the actuator at trial 220 (fuchsia bar) and reinserting (blue bar) at trial 270. Apparent
 600 delay in performance is caused by 50-trial averaging.

601 C. Performance for an example session with stimulus rotation (GO sequence versus square wave
 602 discrimination). Main symbols as for B. Stimuli were delivered, as normal, first in the rostro-caudal
 603 axis (RC; blue bar) but following a brief period of stimulator removal (fuchsia bar), in the dorso-

- 604 ventral (DV; cyan) axis for 50 trials. Stimulation then returned to RC for the remainder of the
605 session.
- 606 D. Lick time raster plot for GO trials in an example session on the final stage of training (GO vs ‘full’
607 NO-GO). Licks are referenced to the start of the sequence, which lasts 800 ms (blue bar). The
608 response period opens at 1 s (purple bar). Water was only available in the response period. Hit
609 and miss trials are green and red dots, respectively.
- 610 E. Lick time raster plot for NO-GO trials of same session as D. Grey-blue bar, sequence. Green dots
611 denote correct rejection trials, red dots false alarm trials.
- 612 F. Smoothed average of lick signals per trial from D and E. Blue, GO trials; grey-blue, NO-GO.
- 613 G. Performance across 8 successive behavioural sessions for one mouse. Performance averaged over
614 a 50-trial moving window.
- 615 H. Hit and false alarm rates as a function of % correct. Each dot, one session on GO vs full NO-GO.
616 The same sessions are depicted in H1 and H2.
- 617

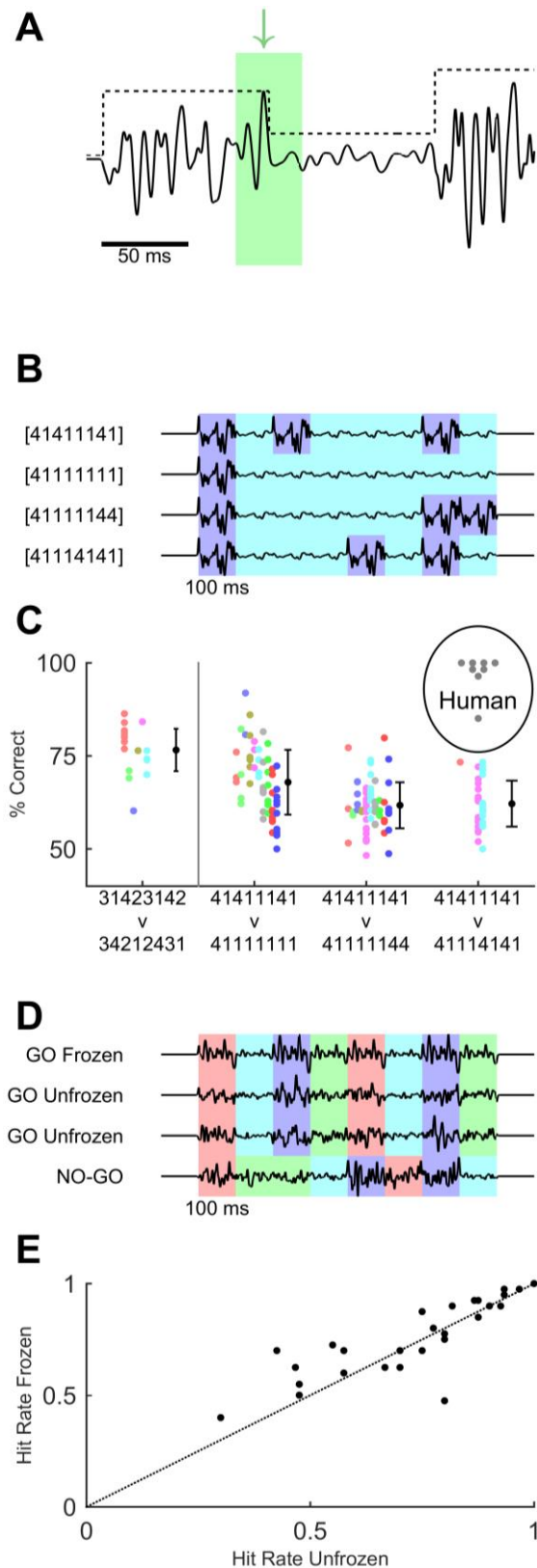


618

619 **Figure 3. Sequence learning performance in humans.**

620 A. Performance over the course of the first training session, measured as % correct averaged over
621 50-trial moving window. Grey lines, individual participants. Black line, average over participants.
622 B. Performance for best 50-trial window on initial test session after training and (on a subset of
623 participants) upon retesting after a minimum of one week. Each grey dot, one participant; black
624 dots, participants tested on both sessions. Dots are jittered along x axis for visualisation.

625



626

627 **Figure 4. Variations of task design to test for behavioural use of cues.**

628 A. Cues within the GO sequence (black line) that could allow recognition of sequence identity. An
629 example of a local cue (within green box) is the large isolated transient “landmark” (green
630 arrow) immediately followed by a low amplitude syllable. In contrast, global cues involve

- 631 changes in integrated stimulus amplitude over time, as reflected in the amplitude modulation
632 envelope (black dotted line).
- 633 B. Binary sequences distinguishable based on syllable ordering or the durations of small-amplitude
634 epochs. Different colours indicate epochs of large and small noise amplitude.
- 635 C. Performance on task variants using binary sequences, compared to original GO vs full NO-GO
636 design (leftmost data point). Each coloured dot indicates a single mouse and session: different
637 mice are in different colours. Black dots and error bars, grand average and SD for each task. Each
638 grey dot indicates performance of an individual human participant on [4 1 4 1 1 1 4 1] vs [4 1 1 1
639 4 1 4 1].
- 640 D. Sequences used to test effect of fixed “landmarks”. Frozen GO used an identical waveform
641 across syllables, trials and sessions. Unfrozen GO maintained the same sequence of noise
642 amplitudes (indicated by colour coding) but varied the detailed waveform across syllables, trials
643 and sessions. NO-GO scrambled the order of syllables, i.e. the sequence of noise amplitudes.
- 644 E. Hit rate of humans on frozen and unfrozen GO trials. Each dot, one participant and session.

645

646